Analytica Chimica Acta: X 5 (2020) 100050

Contents lists available at ScienceDirect

Analytica Chimica Acta: X

journal homepage: www.journals.elsevier.com/analytica-chimica-acta-x

# Oligonucleotide hybridization with magnetic separation assay for multiple SNP phasing

Henson L. Lee Yu , Tsz Wing Fan , I-Ming Hsing *

*Department of Chemical and Biological Engineering, The Hong Kong University of Science and Technology, Clear Water Bay, Kowloon, Hong Kong*

ARTICLE INFO

*Article history:*
Received 11 December 2019
Received in revised form
9 April 2020
Accepted 14 April 2020
Available online 15 April 2020

*Keywords:*
Multiple SNP Phasing
DNA probe Hybridization
Magnetic separation assay
DNA self-Assembly

ABSTRACT

Since humans have two copies of each gene, multiple mutations in different loci may or may not be found on the same strand of DNA (i.e., inherited from one parent). When a person is heterozygous at more than one position, the placement of these mutations, also called the haplotype phase, (i.e., *cis* for the same strand and *trans* for different strands) can result in the expression of different amount and type of proteins. In this work, we described an enzyme-free method to phase two single nucleotide polymorphisms (SNPs) using two fluorophore/quencher-labelled probes, where one of which was biotinylated. The fluorescence signal was obtained twice: first, after the addition of the labelled probes and second, after the addition of the magnetic beads. The first signal was shown to be proportional to the total number of SNP A and SNP B present in the target analyte, while the second signal showed a marked decrease of the fluorescence signal from the non-biotinylated probe when the SNPs were in *trans*, showing that the probe immobilized on the magnetic bead selectively captures targets with SNPs in a *cis* configuration. We then mimic the nature of the human genome which consists of two haplotype copies of each gene, and showed that 250 nM of the 10 possible pairs of haplotypes could be differentiated using a combination of fluorescence microscopy and fluorescence detection.



## 1. Introduction

In the human genome, there are single nucleotide polymorphisms or SNPs in approximately every three hundred bases [1]. Since humans are diploid organisms, multiple SNPs can be inherited together and thus appear in one strand of DNA, or inherited from both parents separately so they appear in different copies of the same gene. Whether the SNPs occur *cis*- or *trans*-with each other, also known as the haplotype phase information, is important since some mutations can mask deleterious effects of another when they occur *cis* to each other [2]. For example, thrombophilia is associated to two mutation sites in the methylenetetrahydrofolate reductase (MTHFR), C677T and A1298C. However, it is only when these two mutations occur *trans* to each other will the diseased phenotype be observed [3]. On other cases, the effects are compounded when the mutations are *cis* with each other such as that for two independent SNPs related to lung cancer and Parkinson's disease [4–6].

Despite the importance of haplotype information, routine DNA sequencing cannot differentiate between *cis* and *trans* SNPs, since the initial DNA target is being fragmented prior to the determination of sequence [7]. Conventionally, when the phase information is required, the DNA from both parents and the patients will be sequenced (called 'trio sequencing') [8–10] and the data will be further analyzed using powerful bioinformatics software [11–13], or when the DNA material from parents are not available, a second sequencing step (i.e, Sanger sequencing) is employed [14].

Recent studies to improve the technology for haplotyping rely on single molecule sequencing, where the sample is repeatedly diluted until only one DNA molecule is isolated in a droplet. In this way, when mutations are detected, they can be unambiguously mapped to a single copy of the DNA, and the haplotype phase can be resolved [15,16]. However, this requires labor-intensive protocols, and needs a high-power computing device for data analyses. Thus, a possible alternative is to use nucleic acid probes to directly obtain phase information.

Direct oligonucleotide hybridization assays are good alternatives and are a simple method to detect mutations, but these are typically limited to identifying the presence of SNPs since, even in multiplexed detection platforms, the observable signal only gives a

* Corresponding author.
*E-mail address:* kehsing@ust.hk (I.-M. Hsing).

https://doi.org/10.1016/j.acax.2020.100050

quantitative information of the mutations present. This is insufficient for phasing studies, because regardless whether the mutations are in *cis* or in *trans*, the signal level generated would be similar since only the placement or the distribution of the SNPs are different, but the total number of SNPs are the same. Further design is therefore required to provide spatial information of the mutation in the genome. In most previous studies that employ DNA hybridization methods to phase haplotypes, the extra step added is usually in the form of iterative testing. For example, Pont-Kingdon et al. determined whether two mutations (R117H and IVS-8) in the Cystic Fibrosis Transmembrane Regulator gene is found in the same DNA strand or not through multiple iterative rounds of allele-specific PCR followed by sequencing of the products generated. This was important because the patient will develop a more severe phenotype if the mutations occur *cis* to each other [17].

Recently, we have shown a DNA self-assembly-based assay, named as conditional displacement hybridization assay, which can be used for the phasing of two SNPs [18]. This was done via a two-step reaction, in which the first step consists of interrogating the presence of SNPs using fluorescently-labelled probes, and the second step is the addition of a DNA polymerase. The enzyme conditionally displaces one of the probes if the SNPs are arranged in *cis*-configuration, and can then be translated to an observable reduction of fluorescence signal. However, the use of an enzyme limits the range of conditions allowable wherein the test can be used. The pH, temperature, ionic strength, and the presence of inhibitors must all be within the optimum values of the enzyme to ensure its activity.

Here, we show an enzyme-free probe hybridization method to provide phase information of two SNPs using the fluorescence signal information before and after magnetic separation. This eliminates the use of multiple iterative testing where separate reaction vessels are required for the same sample to test different haplotypes, and increase the robustness of the detection platform by incorporating a conditional magnetic separation step in lieu of the addition of an enzyme. This enzyme-free approach can be used to obtain the haplotype information of all 10 different pairs of haplotype, also called diplotypes, without the need to consider the operation conditions required for enzyme-based methods.

## 2. Materials and methods

### 2.1. DNA oligonucleotides preparation

The target strands were obtained from Integrated DNA Technologies (IDT), while the rest of the shorter oligonucleotides used were purchased from Sangon Biotech (Shanghai, China). All oligonucleotides were re-suspended in 1X TE buffer (10 mM Tris, 1 mM EDTA, pH = 8.0, Invitrogen) and stored at 4 °C until further use. The sequences of all the DNA strands used are found in Table S1 (in Supplementary information).

### 2.2. Probe preparation and quantification

Probes used in fluorescence detection were prepared by adding the fluorophore-labelled strand and 1.5 times the amount of quencher strands in 1X TE buffer with 12.5 mM $MgCl_2$. The mixture was first heated to 95 °C and slowly cooled down to 20 °C in a span of 3 h using a thermal cycler (Applied Biosystems, Veriti). The annealed probes were then stored at 4 °C. Quantification of the amount of DNA was done via Nanovue Plus Spectrophotometer (GE Healthcare).

### 2.3. Fluorescence measurement

Real-time fluorescence measurements were performed using Varioskan Lux Multimode Microplate reader (Thermo Scientific). A stock solution composed of 250 nM each of the annealed probes in 1X PBS buffer (diluted from 10X PBS Buffer, Invitrogen) was prepared, and then, 52.5 μl of the stock solution was added onto the black 96-well plates (Corning) without the target DNA strands. The instrument was programmed to measure fluorescence using two channels (Ex/Em = 500/520 nm and 580/605 nm, which corresponds to the excitation and emission $\lambda_{max}$ of FAM and ROX, respectively) for 5 min to obtain the baseline measurements. Lastly, 7.5 μl of the appropriate targets are added, yielding a final volume of 60 μl for each reaction containing 250 nM of the target. The fluorescence signals at the same wavelengths were monitored for another 30 min.

### 2.4. Magnetic bead separation

Magnetic beads (Dynabeads MyOne Streptavidin C1, Invitrogen) were first prepared following manufacturer's instruction. Briefly, 200 μl of the stock beads solution (10 μg/μl) were first washed twice with 1 mL of 2X Bind and Wash (B&W) Buffer (10 mM Tris, 1 mM EDTA, 2 M NaCl, pH = 8), and the supernatant was removed after magnetic separation using DynaMag (Invitrogen) magnetic stand. The final residue was re-dissolved in 200 μl of the 2X BW buffer and stored at 4 °C until further use. Fresh preparation of the magnetic beads is preferred; thus, small batches were prepared as needed.

After the fluorescence measurement, the reaction solution in each well was transferred to a microfuge tube and 15 μl (unless otherwise indicated) of the magnetic bead solution was added, and incubated at 37 °C with mild shaking using the Thermomixer (Multi-Therm, Benchmark) for 30 min (unless otherwise indicated). After which, the magnetic beads were magnetically separated from the mixture, and re-dissolved in 60 μl 1X PBS, and the fluorescence measurements at 500/520 and 580/605 were obtained.

### 2.5. Fluorescence microscope imaging

An aliquot of the re-suspended magnetic beads after incubation with the probe and target was transferred onto a glass plate and secured with a cover slip. The microscope image (40× magnification) was obtained using a fluorescent microscope (Eclipse Ni–U, Nikon). In order to compare the intensity of the green and red fluorescence images, they were all obtained with exactly the same conditions. For images with green filter (Ex:460–490 nm/Em:515 nm), with 300 ms exposure time and analog gain of 1.0x using 90% fluorescent lamp intensity; while images with red filter (Ex: 510–550 nm/Em:590 nm) were obtained using 300 ms exposure time and analog gain of 6.2x using 90% fluorescent lamp intensity.

### 2.6. Statistical treatment of data

Results are presented as the mean of triplicate measurements with standard deviations as error bars. The fluorescence signals of the diplotypes were grouped as two-, one-, or no SNP present, and was compared to each other by one-way ANOVA with Tukey HSD post hoc. Comparison of SNP A signals from cis and trans diplotypes were done by two-tailed Student's T-test. *P* values are indicated in each comparison.

## 3. Results and discussion

### 3.1. Design and scheme of the probe hybridization with magnetic separation assay

An overall illustration of the approach is divided into two parts as shown in Fig. 1 – first, to detect the presence of SNPs A and B, and then, to determine the phase of the SNPs present. In the first part, two initially quenched toehold exchange probes are added, labelled PA and PB, to selectively interrogate the presence of two SNPs, A and B, respectively. For example, when SNP A is present, the fluorophore-modified strand of probe A will hybridize with the target, and produce a red fluorescence signal, while a green signal is produced in a similar process when SNP B is present. The probes used are rationally designed through an online nucleic acid analysis tool, Nupack® [19], such that each probe hybridization reaction has a ΔG near 0. This allows for the optimum discrimination between each SNP and their corresponding wild type counterpart, since a single base mismatch bubble can incur a penalty ΔG of around +4 kcal/mol [20], and thus sufficiently make the reaction thermodynamically unfavorable.

After the first step, we find that the signal intensity of each fluorescence channel is proportional to the amount of the corresponding SNP; i.e., if the target contains one "A" SNP (e.g. target TA), a red signal is observed; and if the target contains one "B" SNP (e.g. target TB), a green signal is observed. If the target contains both SNPs (e.g. target TD), both channels will show a high signal; and lastly, if none of the SNPs are present (e.g. target WT), both channels will show a low or negligible signal (Fig. 1A). When two types of targets are mixed together, to mimic a heterozygous DNA sample, the fluorescence signal from a mixture of TD and WT will be similar to that of TA and TB (Fig. 1B) since both pairs will have a total of one SNP A (from TD in the first pair, and TA in the second), and one SNP B (also from TD in the first, and TB in the second). As such, a second step is required to differentiate the two.

One of the probes (PB) is biotinylated on one strand, so that upon the addition of a streptavidin-coated magnetic bead in the second step, PB will be immobilized onto the bead, and consequently, when the targets with SNP B (i.e, TD and TB) hybridize with the probe PB, they will also be linked to the bead. Similarly, since the fluorescently-labelled strand of probe A is hybridized to the TD strand, the red fluorophore will also be dragged to the solid phase retentate upon magnetic separation, if and only if the sample contains a TD molecule. This enables the differentiation of the *cis* (TD and WT) the *trans* (TA and TB) diplotypes (Fig. 1C).

Probe B was chosen to be biotinylated in the 3′ position despite the final product structure having the magnetic bead attaching to the middle of the target rather than at the 5' end (Fig. 1C) since there was negligible difference in the capture efficiency of probe regardless of the position of the biotin group and the design shown exhibited the highest selectivity based from in silico thermodynamic calculations (data not shown).

### 3.2. Detection of SNPs on single-strand targets

The first part of the scheme was tested on 250 nM probe concentrations with equimolar target strands, and the average of triplicate real-time fluorescence measurements is shown in Fig. 2A and B for SNPs A and B respectively.

Fig. 2A is smoothened using box average of 3 consecutive signals in order to remove the noise from the instrument, which caused significant fluctuations particularly at the wavelength corresponding to the ROX fluorophore (see Fig. S1A for the fluorescence signals prior to any processing of the data). The graphs show that the values reach a plateau in less than 10 min, indicating that both probe hybridization reactions occur very fast, and are stable for at least 30 min (see Figs. S1A and S1B).

We also confirmed the selectivity of the probe hybridization

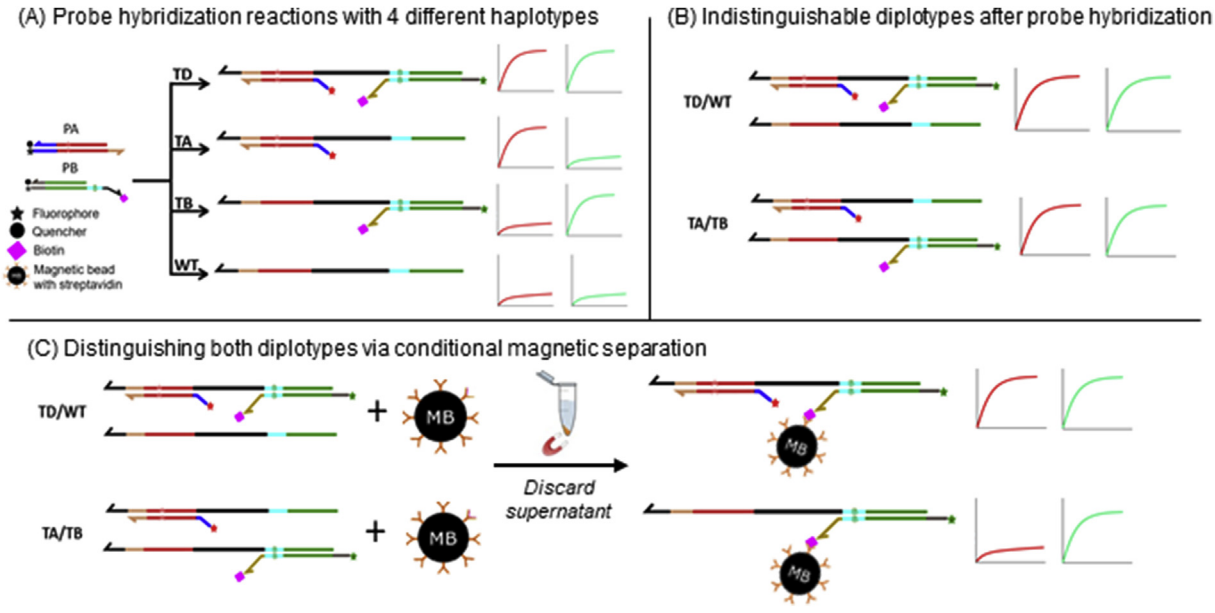


**Fig. 1.** Schematics of the magnetic bead-mediated SNP phasing assay. (A) Two probes labelled PA and PB are designed to interrogate two SNPs, SNP A and SNP B, from any of the four targets: TA – target containing SNP A, TB – target containing SNP B, TD – target containing both SNPs A and B, or WT – target containing none of the SNPs. The first step involves the specific hybridization of the toehold probes yielding a red or green fluorescence signal due to the presence of SNP A or B, respectively. In cases where diplotypes are added, i.e., a mixture of any two out of the four targets mentioned above, the intensity of the signal is proportional to the number of SNPs present – 0, 1, or 2. (B) At this step, two diplotypes cannot be differentiated because of similar fluorescence profile. (C) Differentiation strategy of the two diplotypes TD + WT and TA + TB, both of which contains 1 SNP A and 1 SNP B. Since only the probe PB is biotinylated, when the magnetic bead (MB) is added, only samples with TD and TB can be magnetically separated. Moreover, since TD contains both SNPs A and B, the retentate will also yield a red fluorescence. By measuring the intensity of the red signal after magnetic separation, the TD + WT diplotype can be differentiated from the TA + TB diplotype.

reactions to differentiate single-base mutants for both SNPs A and B, albeit with different degrees of selectivity. For example, comparing Fig. 2A and B, probe B exhibited lower selectivity as shown from the ratio of the signals generated from the mismatched target over the perfectly matched target. This is due to the varying ΔG difference caused by a mismatched base pair. Despite this, the fluorescence signals from the 10 diplotypes can be unambiguously grouped into three: above 1.62 which corresponds to having 2 SNP alleles present, 1.02–1.25 for those with 1 SNP present, and below 0.63 for the rest without any SNP present (Fig. 2C). Each group was also shown to be statistically different from each other, thereby confirming that the different types of diplotypes can be identified from the intensity of the signals.

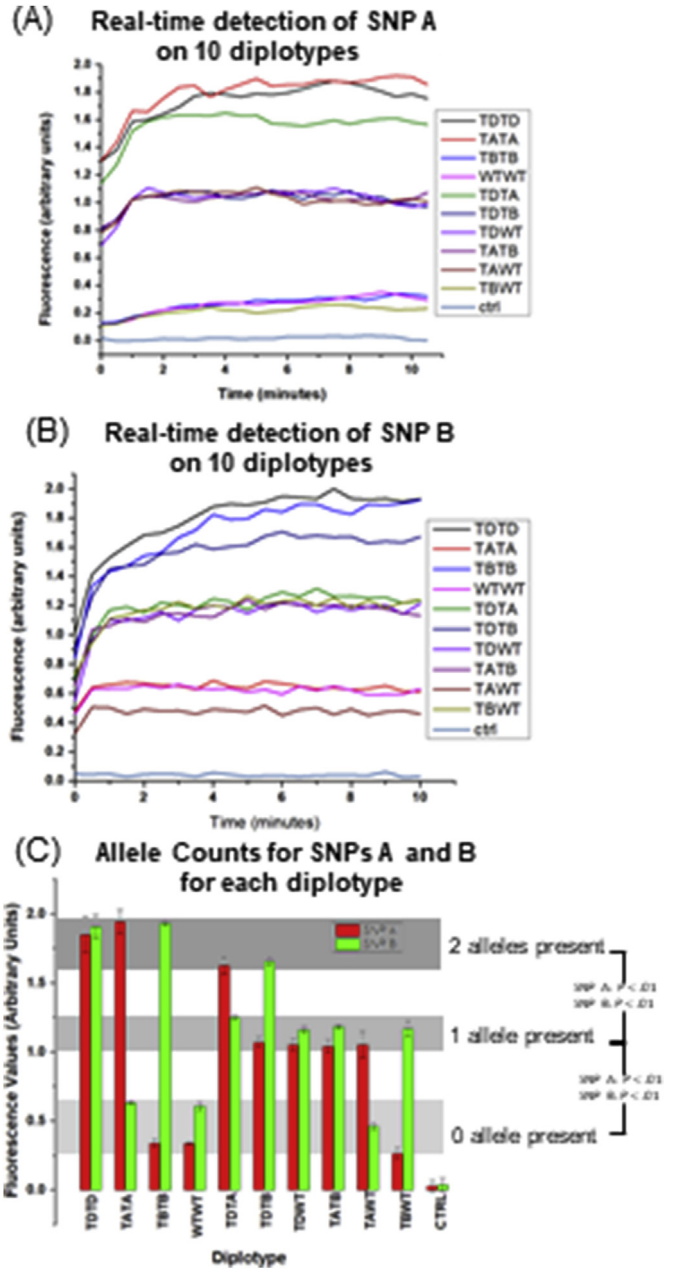


**Fig. 2.** Fluorescence readout for all 10 diplotypes prior to magnetic separation. Real-time measurements of fluorescence values for (A) SNP A and (B) SNP B were simultaneously obtained using a microplate reader of the 10 diplotypes Graphs show rapid kinetics, with equilibrium values reached in less than 10 min. Normalized equilibrium values for each trial were averaged and summarized in (C), and the fluorescence readings above 1.6 correspond to 2 alleles, between 1.0 and 1.2 correspond to 1 allele, and values below 0.6 correspond to no SNP allele present. ($P < 0.01$ for both SNPs A and B, one-way ANOVA with Tukey HSD post hoc analysis). Error bars represent the standard deviation from triplicate measurements. TD: two SNPs are present, TA: only SNP A is present, TB: only SNP B is present, and WT: none of the SNPs are present. Each reaction contains two of the four targets, named by combining the two symbols together (TDTD = two TD's present, TDTA = one TD and one TA, etc.).

### 3.3. Efficiency of magnetic bead (MB) capture

Since TD/WT and TA/TB both contain one SNP A and one SNP B each, a conditional separation step is employed to resolve the two diplotypes. Despite the wide use of streptavidin-coated magnetic beads in separation and capture of biotinylated DNA probes [21–23], the capture efficiency would have to be optimized for this specific assay to take into account the properties known to affect the immobilization thermodynamics and kinetics such as the length and secondary structure of the target [24], salt concentration and ionic strength [25], length of spacer nucleotides (between biotin and the toehold region) [26], etc. We find that the most significant factor in this work was the probe density as calculated

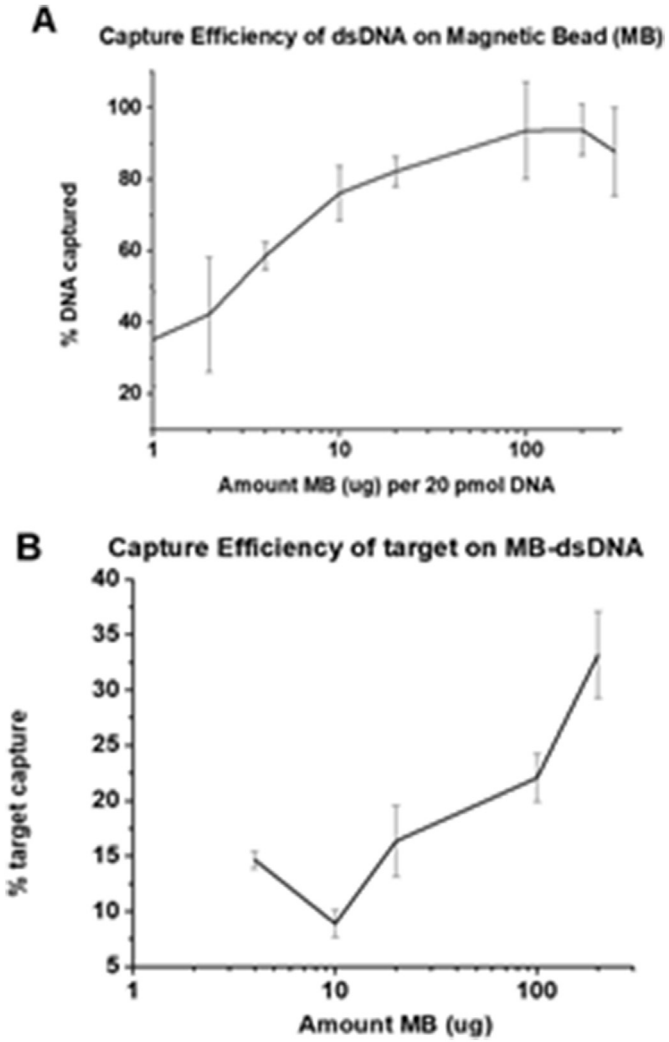


**Fig. 3.** Efficiency of capture of (A) dsDNA probes onto magnetic beads showing that MB is saturated with PB at 100 μg MB per 20 pmol DNA (>90% immobilized); (B) but more target DNA strand can be hybridized onto the MB-dsDNA conjugate, when lower probe density (i.e., more MB is added) is used. Error bars represent the standard deviation from triplicate measurements.

from the ratio of magnetic bead and the biotinylated probe, assuming even distribution of the probes onto the magnetic bead.

Fig. 3A shows the change in capture efficiency (defined as the amount of double-stranded probe captured/total amount of probe added), and the results show that more than 90% of the dsDNA are captured when a ratio of 5 μg MB is added for every pmol of dsDNA. In contrast, <10% of a non-biotinylated DNA probe was captured, signifying negligible non-specific binding to the MB (see Table S2).

While the streptavidin-biotin interaction is rapid and stable, when the probe density is too high, it will limit the capture of a 150-mer target DNA due to steric hindrance and ionic repulsion. Thus, the amount of target (TD) that can be immobilized was also optimized. This was done by first adding different mixtures of MB-probe B (MB-PB) conjugate, and magnetically separate to remove all of the unbound PB strands. Then, the MB-PB retentate was re-suspended in a 1X PBS solution with 20 pmol TD followed by 1 h incubation with moderate shaking.

Fig. 3B shows the amount of TD captured by measuring the $OD_{260}$ value of the supernatant and corrected to subtract the amount of the quencher strand released as a byproduct of the reaction. The best conditions were obtained when 10 μg of MB: 1 pmol DNA strand ratio was used, which translates to $10^4$ DNA molecules per MB or a surface coverage of $3 \times 10^{12}$ DNA particles per $cm^2$ of MB, and resulted to 33% of the TD strand being hybridized. The optimal surface density and probe capture efficiency is in agreement with the ones reported previously [24,25].

### 3.4. Fluorescence microscopy images of magnetic beads

Since the target immobilization onto the MB-PB conjugate is a strand displacement reaction, wherein a quencher strand is released upon the hybridization of the target, this process will yield a fluorescently-labelled beads which can be viewed under a microscope, with the appropriate filters. Fig. 4 shows the microscope images when different targets are added to the MB-PB conjugate and the subsequent addition of PA after washing the unbound target strands (incubated for 1 h at 37 °C). The fluorescence intensity is then compared with the fluorescence signal of the probe B without target. (see Fig. S2 for the difference in the background signal as different ratios of the fluorophore and quencher strand were used to prepare the probe PB).

Brighter images were obtained when perfectly complementary probe and target pair was added, although the contrast between positive green signals (TD and TB) and negative ones (TA and WT) is limited by the same reaction ΔG difference discussed earlier. For the red signal, only TD is expected to have bright red signal because a washing step was added prior to the addition of probe PA.

### 3.5. Fluorescence measurement after conditional separation

Because it would be difficult to differentiate the fluorescence intensity produced from one allele with that of two alleles through microscope images alone, and the direct quantification of the fluorescence values of the green signal during hybridization produced 25% less as compared to its homogeneous counterpart (Fig. S3), the overall scheme was designed to first allow the two probes (PA and PB) to hybridize with the target prior to the addition of magnetic bead, and re-quantify the red fluorescence signal of the retentate after 30 min incubation. Less time is needed since the hybridization reaction between the probes and the targets are completed.

Fig. 5 shows the normalized values of the equilibrium fluorescence signals corresponding to the ROX fluorophore (Ex/Em 580/605 nm) where the highest is set at 2, corresponding to two alleles

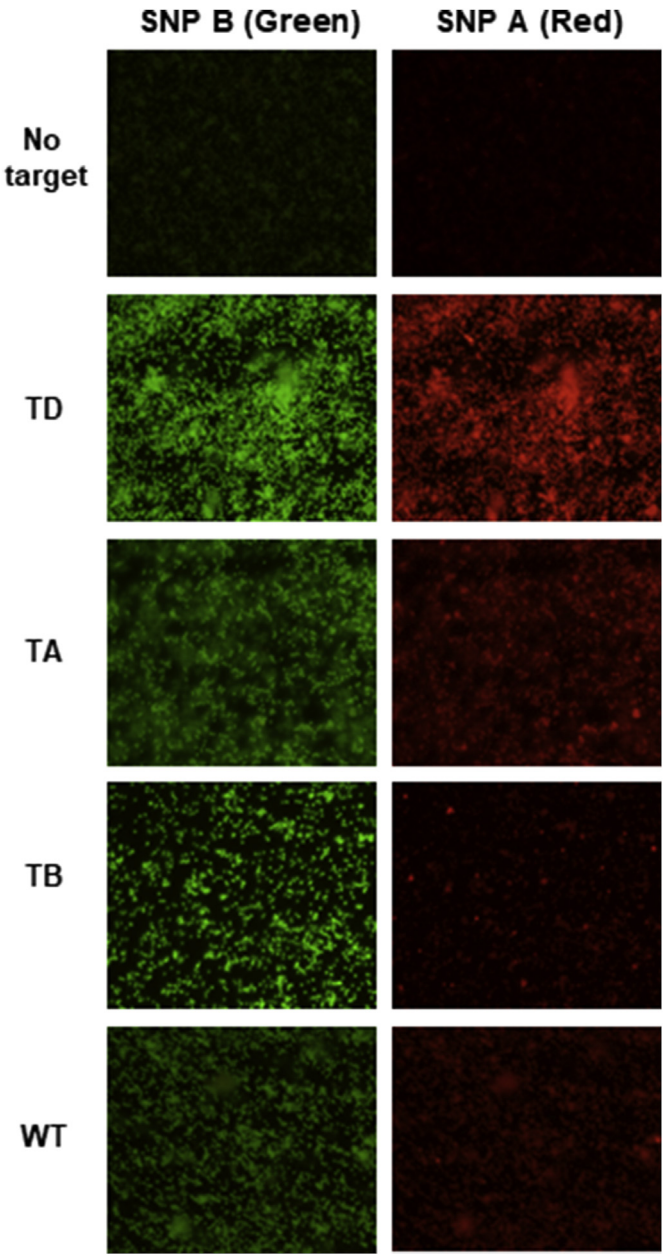


**Fig. 4.** Fluorescence images of the MB after stepwise addition of PB, then the corresponding target (except for the no target control), and then with PA. Each incubation step was done for 1 h at 37 °C with moderate shaking. All images were obtained with similar magnification, light intensity, and exposure time. Green filter showed brighter intensity for TD and TB since both contains SNP B, while the red filter showed brighter intensity for TD only since PA will only be immobilized to the MB when TD is present.

of SNP A retained, as in the case of a homozygous TD/TD diplotype. This was followed by the three heterozygous diplotypes containing TD (TDTA, TDTB, and TDWT), although the signal from TDTB was consistently slightly lower from the other two, presumably because less TD can be captured due to the electrostatic repulsion with TB also immobilized onto the MB. Similarly, TATB and TBWT have lower signal from TAWT since the TB being captured to the magnetic bead prevented probes with TA from being retained as well. This generates a much more significant difference between TDWT and TATB, which are the two diplotypes previously not differentiable using the homogeneous probe hybridization step as seen in Fig. 1C.

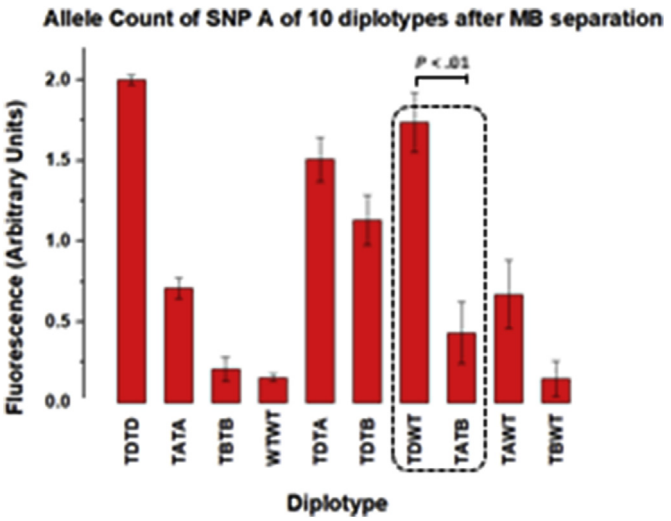


**Fig. 5.** Red signal of the 10 diplotypes after magnetic separation. The enclosed signals show that the *cis* (TDWT) and *trans* (TATB) SNPs can be unambiguously differentiated. ($P < 0.01$, independent student's t-test, two-tailed) Error bars represent the standard deviation from triplicate measurements.

## 4. Conclusion

In summary, we designed herein a molecular method to phase two SNPs that eliminates the use of iterative probe hybridization steps by combining rationally-designed nucleic acid reactions with a magnetic separation step. A key improvement in this work is the absence of an enzyme leading to a more robust design, without the need for optimal temperature, buffer, and other conditions required for enzyme activity. The sensitivity in this work is also not optimized, and we used 15 pmol of unamplified sample. Although the signal can be amplified to reduce the limit of detection by 4–5 orders of magnitude [27,28], care must be taken that the range of the fluorescence signals that correspond to the number of each allele present (2, 1, or 0 for each SNP) must not overlap in order to achieve a conclusive haplotype phasing. This can be improved by incorporating an amplification step such as PCR similar to previously reported methods [29–32] (see Table S3 in supplementary information).

Although next-generation sequencing and computational approaches to phasing will be more powerful in determining haplotypes since theoretically, it is not limited by the number of SNPs and it can be used for de novo SNP discovery and phasing, this method offers a direct method for phasing of two SNPs already associated to some altered disease risk or severity. Furthermore, this method has a potential for multiple SNP diagnostics and phasing by incorporating more probes with different fluorophores.

## Declaration of competing interest

The authors declare that they have no known competing financial interests or personal relationships that could have appeared to influence the work reported in this paper.

## CRediT authorship contribution statement

**Henson L. Lee Yu:** Methodology, Investigation, Data curation, Writing - original draft. **Tsz Wing Fan:** Conceptualization. **I-Ming Hsing:** Supervision, Writing - review & editing.

## Acknowledgments

We thank the Research Grants Council of the Hong Kong SAR Government for the funding support (grant # GRF 16306218). HLY and TWF acknowledge the fellowship support from the Hong Kong Ph.D. Fellowship Scheme (HKPFS).

## Appendix A. Supplementary data

Supplementary data to this article can be found online at https://doi.org/10.1016/j.acax.2020.100050.

## References

[1] S. Browning, B. Browning, Haplotype phasing: existing methods and new developments, Nat. Rev. Genet. 12 (2011) 703–714, https://doi.org/10.1038/nrg3054.Haplotype.
[2] M.R. Hoehe, G.M. Church, H. Lehrach, T. Kroslak, S. Palczewski, K. Nowick, S. Schulz, E.-K. Suk, T. Huebsch, Multiple haplotype-resolved genomes reveal population patterns of gene and protein diplotypes, Nat. Commun. 5 (2014) 1–12, https://doi.org/10.1038/ncomms6569.
[3] N.M. Brown, V.M. Pratt, A. Buller, L. Pike-Buchanan, J.B. Redman, W. Sun, R. Chen, B. Crossley, M.J. McGinniss, F. Quan, C.M. Strom, Detection of 677CT/1298AC "double variant" chromosomes: implications for interpretation of MTHFR genotyping results, Genet. Med. 7 (2005) 278–282, https://doi.org/10.1097/01.gim.0000159904.92850.d5.
[4] R. Pan, P. Xiao, Quantitative haplotyping of PCR products by nonsynchronous pyrosequencing with di-base addition, Anal. Bioanal. Chem. 408 (2016) 8263–8271, https://doi.org/10.1007/s00216-016-9936-7.
[5] Y.R. Wu, K.H. Chang, W.T. Chang, Y.C. Hsiao, H.C. Hsu, P.R. Jiang, Y.C. Chen, C.Y. Chao, Y.C. Chang, B.H. Lee, F.J. Hu, W.L. Chen, G.J. Lee-Chen, C.M. Chen, Genetic variants of LRRK2 in Taiwanese Parkinson's disease, PloS One 8 (2013) 11–14, https://doi.org/10.1371/journal.pone.0082001.
[6] Y. Wang, H. Liu, N.E. Ready, L. Su, Y. Wei, D.C. Christiani, Q. Wei, Genetic variants in ABCG1 are associated with survival of non- small cell lung cancer patients, Int. J. Canc. 138 (2016) 2592–2601, https://doi.org/10.1016/j.physbeh.2017.03.040.
[7] R. Lippert, R. Schwartz, G. Lancia, S. Istrail, Algorithmic strategies for the single nucleotide polymorphism haplotype assembly problem, Briefings Bioinf. 3 (2002) 23–31, https://doi.org/10.1093/bib/3.1.23.
[8] J. O'Connell, D. Gurdasani, O. Delaneau, N. Pirastu, S. Ulivi, M. Cocca, M. Traglia, J. Huang, J.E. Huffman, I. Rudan, R. McQuillan, R.M. Fraser, H. Campbell, O. Polasek, G. Asiki, K. Ekoru, C. Hayward, A.F. Wright, V. Vitart, P. Navarro, J.F. Zagury, J.F. Wilson, D. Toniolo, P. Gasparini, N. Soranzo, M.S. Sandhu, J. Marchini, A general approach for haplotype phasing across the full spectrum of relatedness, PLoS Genet. 10 (2014), https://doi.org/10.1371/journal.pgen.1004234.
[9] R. Tewhey, V. Bansal, A. Torkamani, E.J. Topol, N.J. Schork, The importance of phase information for human genomics, Nat. Rev. Genet. 12 (2011) 215–223, https://doi.org/10.1038/nrg2950.
[10] J.C. Roach, G. Glusman, R. Hubley, S.Z. Montsaroff, A.K. Holloway, D.E. Mauldin, D. Srivastava, V. Garg, K.S. Pollard, D.J. Galas, L. Hood, A.F.A. Smit, Chromosomal haplotypes by genetic phasing of human families, Am. J. Hum. Genet. 89 (2011) 382–397, https://doi.org/10.1016/j.ajhg.2011.07.023.
[11] J. Marchini, D. Cutler, N. Patterson, M. Stephens, E. Eskin, E. Halperin, S. Lin, Z.S. Qin, H.M. Munro, G.R. Abecasis, P. Donnelly, A comparison of phasing algorithms for trios and unrelated individuals, Am. J. Hum. Genet. 78 (2006) 437–450, https://doi.org/10.1086/500808.
[12] B.L. Browning, Z. Yu, Simultaneous genotype calling and haplotype phasing improves genotype Accuracy and reduces false-positive associations for genome-wide association studies, Am. J. Hum. Genet. 85 (2009) 847–861, https://doi.org/10.1016/j.ajhg.2009.11.004.
[13] O. Delaneau, C. Coulonges, J.F. Zagury, Shape-IT: new rapid and accurate algorithm for haplotype inference, BMC Bioinf. 9 (2008) 1–14, https://doi.org/10.1186/1471-2105-9-540.
[14] A. Bhattacharjee, T. Sokolsky, S.K. Wyman, M.G. Reese, E. Puffenberger, K. Strauss, H. Morton, R.B. Parad, E.W. Naylor, Development of DNA confirmatory and high-risk diagnostic testing for newborns using targeted next-generation DNA sequencing, Genet. Med. 17 (2015) 337–347, https://doi.org/10.1038/gim.2014.117.
[15] J.O. Kitzman, Haplotypes drop by drop, Nat. Biotechnol. 34 (2016) 296–298, https://doi.org/10.1038/nbt.3500.
[16] C. Ding, C.R. Cantor, Direct molecular haplotyping of long-range genomic DNA with M1-PCR, Proc. Natl. Acad. Sci. U. S. A 100 (2003) 7449–7453, https://doi.org/10.1073/pnas.1232475100.
[17] G. Pont-Kingdon, M. Jama, C. Miller, A. Millson, E. Lyon, Long-range (17.7 kb) allele-specific polymerase chain reaction method for direct haplotyping of R117H and IVS-8 mutations of the cystic fibrosis transmembrane regulator gene, J. Mol. Diagnostics. 6 (2004) 264–270, https://doi.org/10.1016/S1525-1578(10)60520-X.

[18] T.W. Fan, H.L. Lee Yu, I.-M. Hsing, Conditional displacement hybridization assay for multiple SNP phasing, Anal. Chem. 89 (2017) 9961–9966, https://doi.org/10.1021/acs.analchem.7b02300.
[19] J.N. Zadeh, C.D. Steenberg, J.S. Bois, B.R. Wolfe, M.B. Pierce, A.R. Khan, R.M. Dirks, N.A. Pierce, NUPACK : analysis and design of nucleic acid systems, J. Comput. Chem. 32 (2011) 170–179, https://doi.org/10.1002/jcc.
[20] D.Y. Zhang, S.X. Chen, P. Yin, Optimizing the specificity of nucleic acid hybridization, Nat. Chem. 4 (2012) 208–214, https://doi.org/10.1038/nchem.1246.
[21] S. Yue, T. Zhao, S. Bi, Z. Zhang, Programmable strand displacement-based magnetic separation for simultaneous amplified detection of multiplex microRNAs by chemiluminescence imaging array, Biosens. Bioelectron. 98 (2017) 234–239, https://doi.org/10.1016/j.bios.2017.06.060.
[22] R.A. Fenati, D. Khodakov, A.V. Ellis, Optimisation of DNA hybridisation and toehold strand displacement from magnetic bead surfaces, Int. J. Nanotechnol. 14 (2017) 75–86, https://doi.org/10.1504/IJNT.2017.082447.
[23] H. Li, Z. He, Magnetic bead-based DNA hybridization assay with chemiluminescence and chemiluminescent imaging detection, Analyst 134 (2009) 800–804, https://doi.org/10.1039/b819990f.
[24] M.J. Archer, B. Lin, Z. Wang, D.A. Stenger, Magnetic bead-based solid phase for selective extraction of genomic DNA, Anal. Biochem. 355 (2006) 285–297, https://doi.org/10.1016/j.ab.2006.05.005.
[25] A.W. Peterson, R.J. Heaton, R.M. Georgiadis, The effect of surface probe density on DNA hybridization, Nucleic Acids Res. 29 (2001) 5163–5168, https://doi.org/10.1093/nar/29.24.5163.
[26] H. Ravan, S. Kashanian, N. Sanadgol, A. Badoei-Dalfard, Z. Karami, Strategies for optimizing DNA hybridization on surfaces, Anal. Biochem. 444 (2014) 41–46, https://doi.org/10.1016/j.ab.2013.09.032.
[27] H. Hagiwara, K. Sawakami-Kobayashi, M. Yamamoto, S. Iwasaki, M. Sugiura, H. Abe, S. Kunihiro-Ohashi, K. Takase, N. Yamane, K. Kato, R. Son, M. Nakamura, O. Segawa, M. Yoshida, M. Yohda, H. Tajima, M. Kobori, Y. Takahama, M. Itakara, M. Machida, Development of an automated SNP analysis method using a paramagnetic beads handling robot, Biotechnol. Bioeng. 98 (2007) 420–428, https://doi.org/10.1002/bit.
[28] B. Armstrong, M. Stewart, A. Mazumder, Suspension arrays for high throughput, multiplexed single nucleotide polymorphism genotyping, Cytometry 40 (2000) 102–108, https://doi.org/10.1002/(SICI)1097-0320(20000601)40:2<102::AID-CYTO3>3.0.CO;2-4.
[29] N. Von Ahsen, V.W. Armstrong, M. Oellerich, Rapid, long-range molecular haplotyping of thiopurine S-methyltransferase (TPMT) *3A, *3B, and *3C, Clin. Chem. 50 (2004) 1528–1534, https://doi.org/10.1373/clinchem.2004.034751.
[30] O.G. McDonald, E.Y. Krynetski, W.E. Evans, Molecular haplotyping of genomic DNA for multiple single-nucleotide polymorphisms located kilobases apart using long-range polymerase chain reaction and intramolecular ligation, Pharmacogenetics 12 (2002) 93–99, https://doi.org/10.1097/00008571-200203000-00003.
[31] B. Arbeithuber, A. Heissl, I. Tiemann-Boege, Haplotyping: Methods & Protocols, Humana Press, 2017, https://doi.org/10.4103/ijmr.ijmr_1433_17.
[32] G. Pont-Kingdon, E. Lyon, Direct molecular haplotyping by melting curve analysis of hybridization probes: beta 2-adrenergic receptor haplotypes as an example, Nucleic Acids Res. 33 (2005) 1–8, https://doi.org/10.1093/nar/gni090.